SUPPLEMENTARY MATERIALS

Migratory properties of pulmonary dendritic cells are determined by their developmental lineage

Hideki Nakano, Joseph E. Burgents, Keiko Nakano, Gregory S. Whitehead, Cheolho Cheong, Carl D. Bortner and Donald N. Cook

This file includes Supplementary Figures S1 through S5

Figure S1

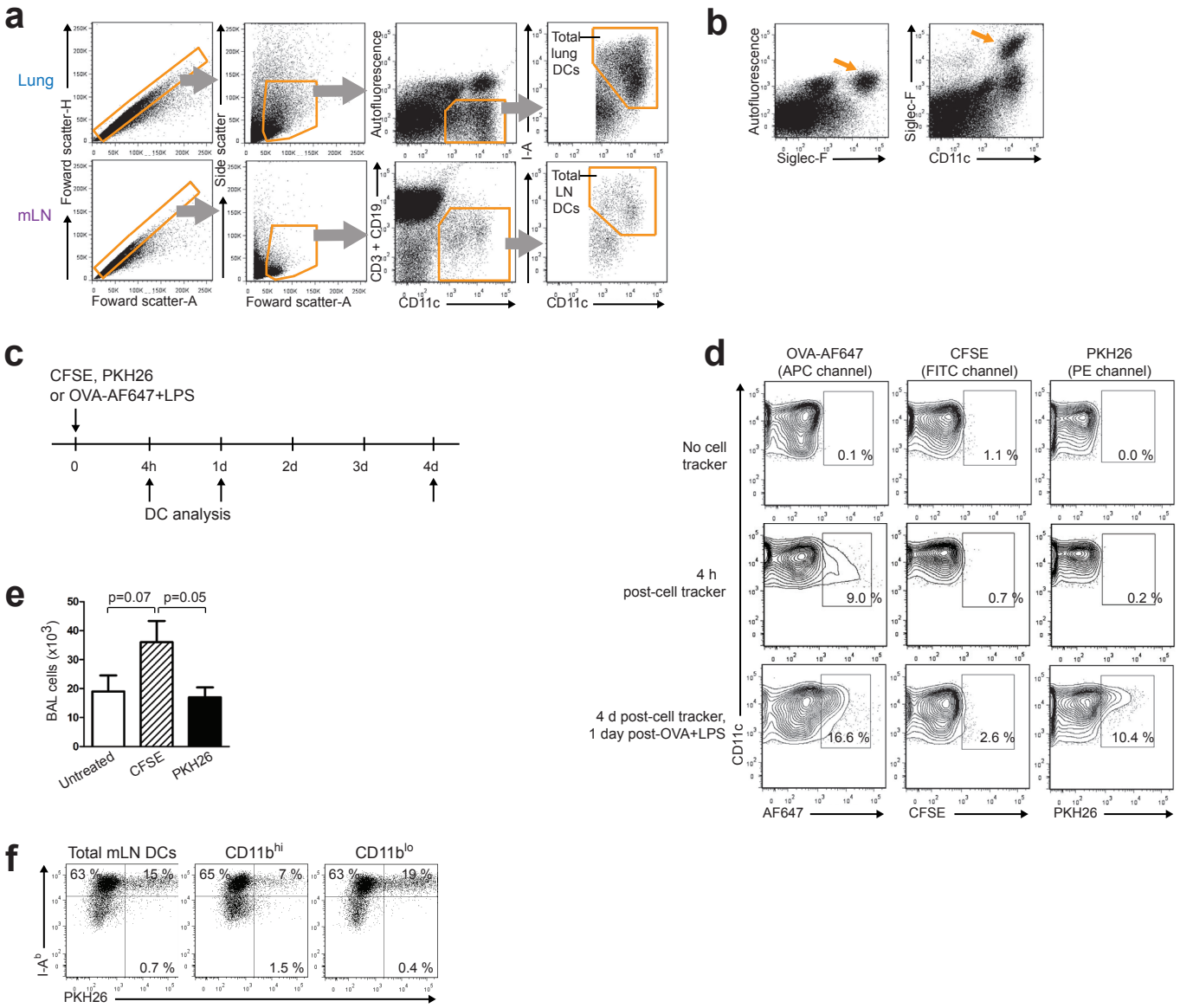
a
Lung
mLN
Foward scatter-H
Foward scatter-A
Side scatter
Autofluorescence
I-A
Total lung DCs
CD3 + CD19
CD11c
Total LN DCs
b
Autofluorescence
Siglec-F
CD11c
c
CFSE, PKH26
or OVA-AF647+LPS
0
4h
1d
2d
3d
4d
DC analysis
d
OVA-AF647 (APC channel)
CFSE (FITC channel)
PKH26 (PE channel)
No cell tracker
4 h post-cell tracker
4 d post-cell tracker, 1 day post-OVA+LPS
0.1 %
1.1 %
0.0 %
9.0 %
0.7 %
0.2 %
16.6 %
2.6 %
10.4 %
CD11c
AF647
CFSE
PKH26
e
p=0.07
p=0.05
BAL cells (x10^3)
Untreated
CFSE
PKH26
f
Total mLN DCs
CD11b^hi
CD11b^lo
63 %
15 %
0.7 %
65 %
7 %
1.5 %
63 %
19 %
0.4 %
I-A^b
PKH26

Supplementary Figure S1. Gating strategy for lung and mLN DCs, and use of fluorescent dyes for tracking DC migration. (**a**) Low density cells from the lung gated on autofluorescence^{lo} I-A^{+}CD11c^{+} cells (top), and low density cells from mLNs gated on CD3^{lo}CD19^{lo}I-A^{+}CD11c^{+} cells (bottom). (**b**) Comparison of autofluorescence and anti-Siglec-F antibody staining to distinguish macrophages from lung DCs. Arrow indicates alveolar macrophages (**c**) Timeline to measure staining of DCs in the lung by CFSE or PKH26, and transport of OVA-AF647 to LNs after DC activation with co-instilled LPS. (**d**) Analysis of stained DCs in mediastinal LNs at the indicated times post-cell tracker and OVA/LPS instillation. (**e**) Airway inflammation induced by instilling CFSE or PKH. Shown are total leukocytes in bronchoalveolar lavage fluid 1 d after instillation of the respective dyes. *P*-value by Mann Whitney test. (*n*=5) (**f**) I-A staining of PKH^{+} mLN DCs.

Figure S2

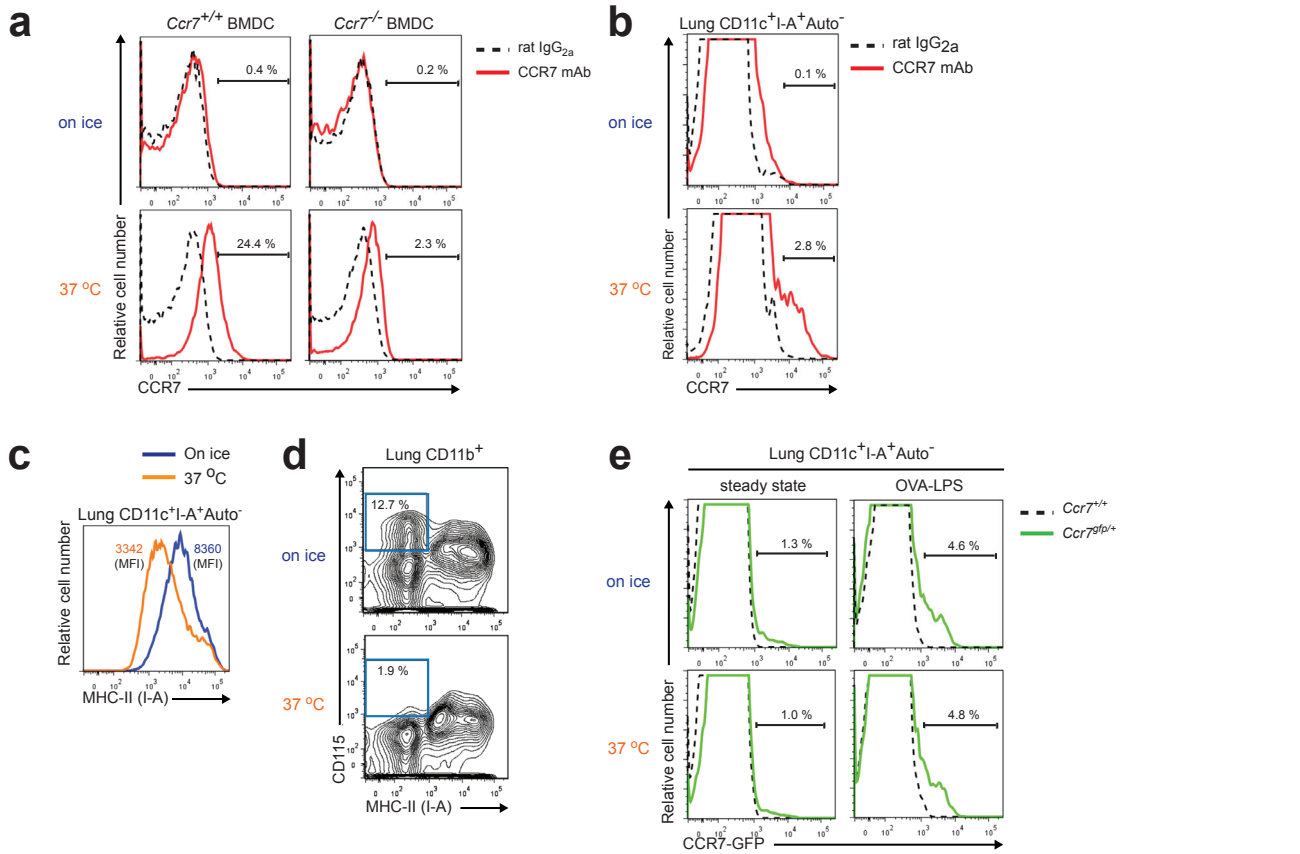

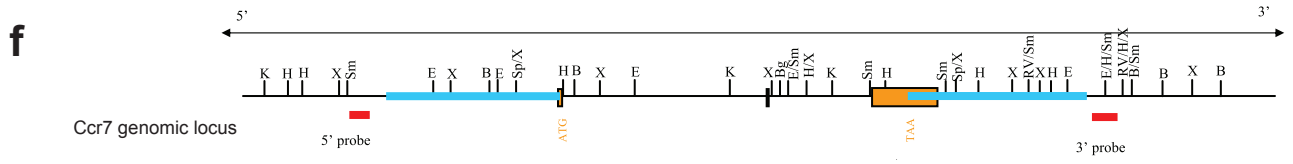

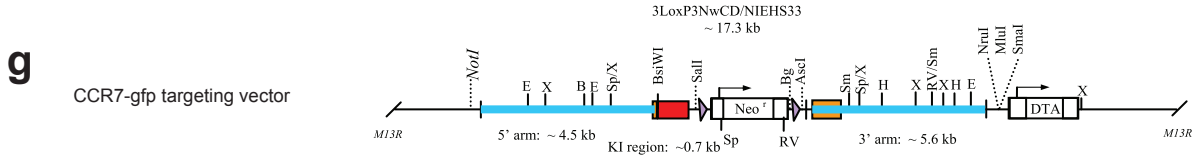

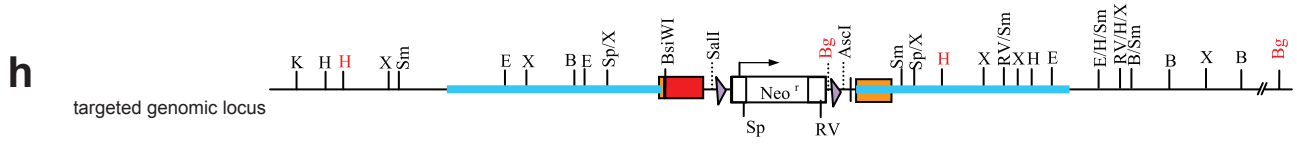

B=BamHI; Bg=BglII; E=EcoRI; H=HindIII; K=KpnI; RV=EcoRV; Sl=Sal I; Sm=SmaI; Sp=Spe1; X=XbaI;

1 kb LoxP site mCCR7 exon GFP cDNA Probe

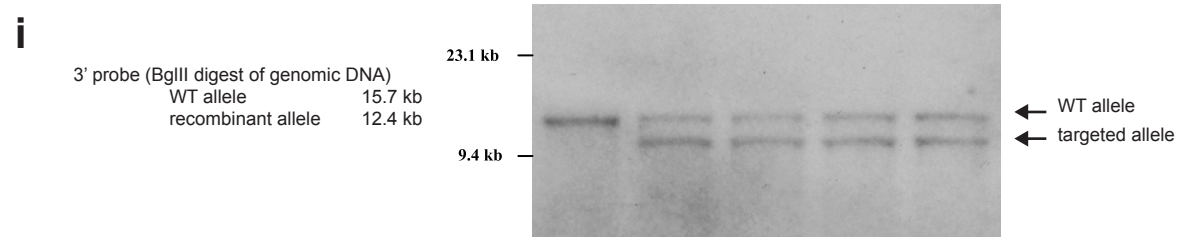

Supplementary Figure S2. Flow cytometric analyses of cells using either anti-CCR7 monoclonal antibodies or *Ccr7*^{gfp} mice, and generation of *Ccr7*^{gfp} reporter mice. (**a**) *In vitro* generated BMDCs (9 days of culture) from wild-type or *Ccr7*$^{-/-}$ mice were stained with PE-labeled anti-CCR7 mAbs on ice or at 37 ^{o}C. Data shown are for gated CD11c^{+}I-A^{+}CD86^{+} cells. (**b**) Lung DCs (CD11c^{+}I-A^{+} autofluorescence^{lo}) from untreated C57BL/6 mice stained with anti-CCR7 mAbs on ice or at 37 ^{o}C. (**c**) MHC class II staining of lung DCs on ice or at 37 ^{o}C. (**d**) Staining for CD115 on I-A^{-}CD11b^{+} monocytes after on ice or at 37 ^{o}C. (**e**) CCR7-GFP fluorescence in lung DCs from untreated *Ccr7*$^{gfp/+}$ mice. (**f**) Structure of the wild-type *Ccr7* locus is shown, with exons in orange, regions used to generate homology in blue. (**g**) Structure of targeting vector. 5' and 3' arms of homology (blue) and GFP coding region (red) are shown. DTA, diphtheria toxin-encoding DNA. (**h**) Structures of targeted *Ccr7* locus. (**i**) Southern blot confirmation of correctly targeted C57BL/6-derived embryonic stem (ES) cells. Neomycin (*neo*)-resistant ES cell colonies were screened by PCR and the expected structure of the targeted locus confirmed by Southern blotting using genomic DNA residing lying outside of the region used to generate arms of homology. The targeted *Ccr7* allele includes the selectable *neo* gene flanked by LoxP sites to allow its deletion from targeted cell lines by *Cre* recombinase. This deletion event was confirmed by PCR-based analysis of genomic DNA following transfection of correctly targeted, *neo*-sensitive cell lines with *cre*-expressing plasmid DNA (data not shown).

Figure S3

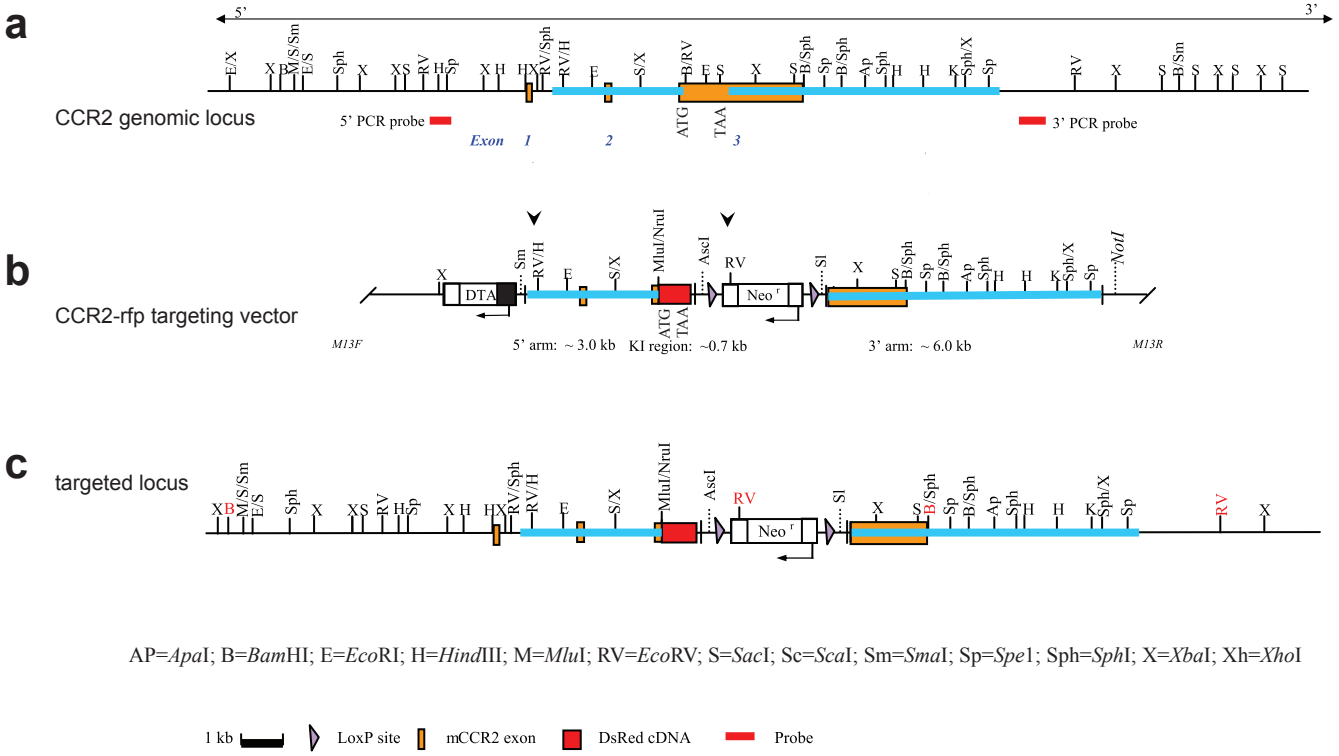
a
CCR2 genomic locus
5'
3'
5' PCR probe
3' PCR probe
Exon 1 2 3
ATG
TAA
b
CCR2-rfp targeting vector
DTA
Neo r
M13F
M13R
5' arm: ~ 3.0 kb
KI region: ~0.7 kb
3' arm: ~ 6.0 kb
c
targeted locus
AP=ApaI; B=BamHI; E=EcoRI; H=HindIII; M=MluI; RV=EcoRV; S=SacI; Sc=ScaI; Sm=SmaI; Sp=Spe1; Sph=SphI; X=XbaI; Xh=XhoI
1 kb
LoxP site
mCCR2 exon
DsRed cDNA
Probe

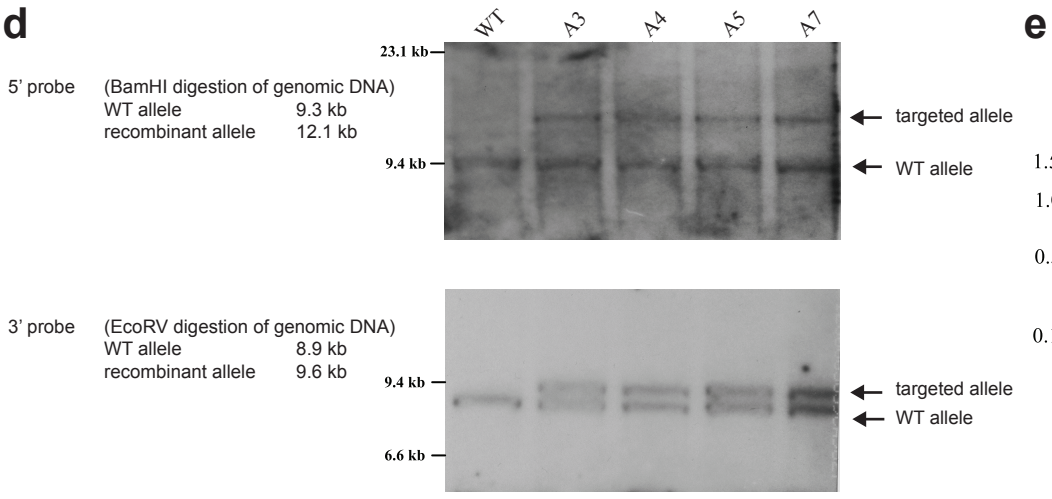
d
5' probe (BamHI digestion of genomic DNA)
WT allele 9.3 kb
recombinant allele 12.1 kb
WT
A3
A4
A5
A7
23.1 kb
9.4 kb
targeted allele
WT allele
3' probe (EcoRV digestion of genomic DNA)
WT allele 8.9 kb
recombinant allele 9.6 kb
9.4 kb
6.6 kb
targeted allele
WT allele

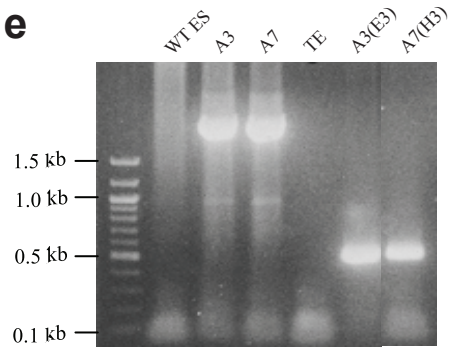
e
WT ES
A3
A7
TE
A3(E3)
A7(H3)
1.5 kb
1.0 kb
0.5 kb
0.1 kb

Supplementary Figure S3. Generation of *Ccr2* null mice. (**a**) *Ccr2* locus with exons in orange and regions of homology in blue. (**b**) Structure of targeting vector. DTA; diphtheria toxin. (**c**) Structure of targeted locus. (**d**) Representative Southern blots showing confirmation of correctly targeted ES cells using 5' and 3' probes. (**e**) PCR-based assay showing *Cre* recombinase-mediated excision of the *neo* gene from two independently targeted ES cell clones. The 2.5 kb band corresponds to the *neo*-containing gene, and the 0.5 kb band corresponds to cells having an excised *neo* gene. In addition to the homology arms, the final vector also contains the *neo* expression cassette (for positive selection of the ES cells) flanked by LoxP sequences (for the subsequent removal of the *neo* cassette), and a DTA expression cassette for negative selection of the ES cells. RFP fluorescence was undetectable in the targeted cells, and the mice were used as non-reporter, gene targeted animals.

Figure S4

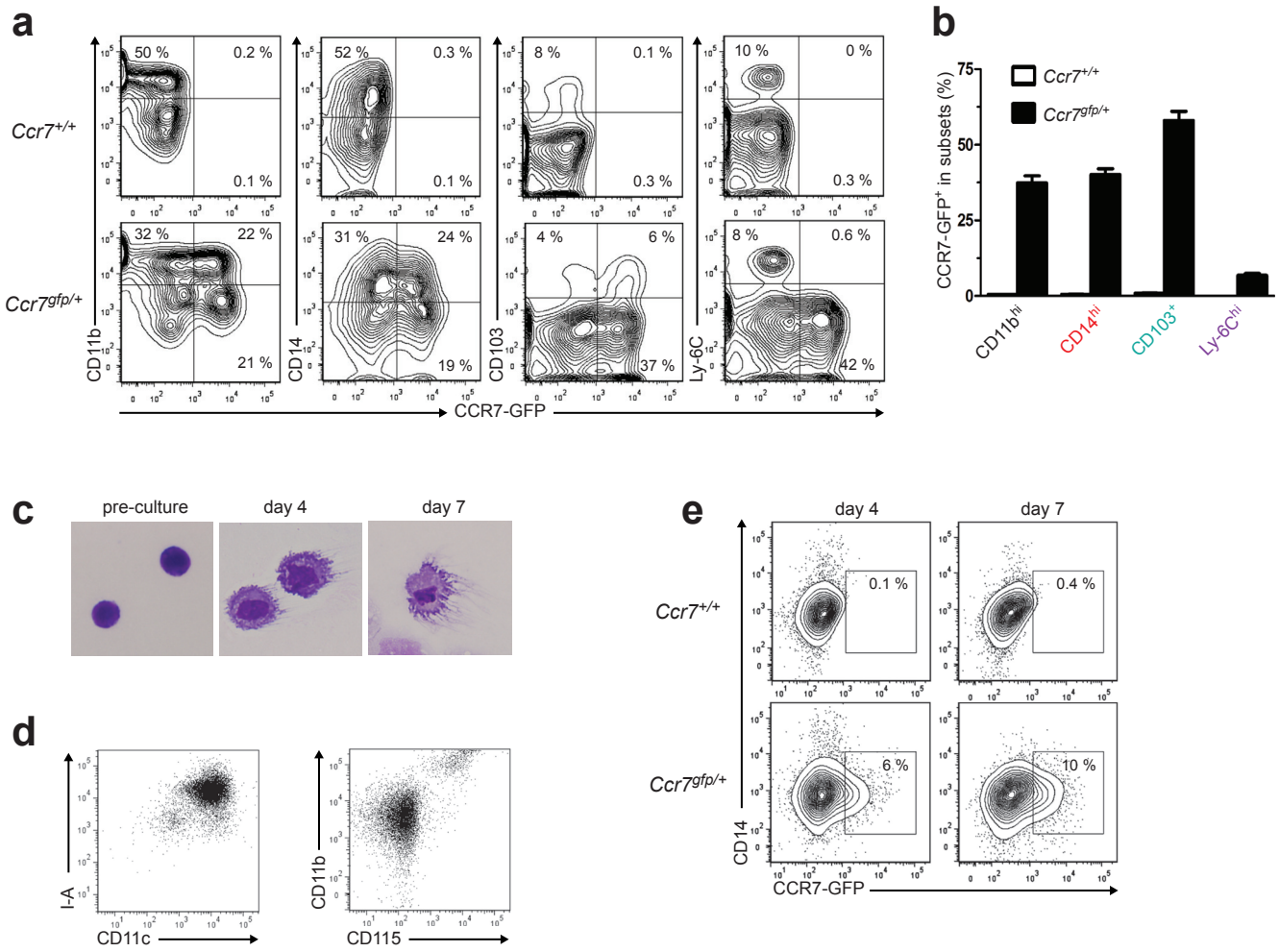
a
Ccr7+/+
Ccr7gfp/+
50 %
0.2 %
0.1 %
32 %
22 %
21 %
52 %
0.3 %
0.1 %
31 %
24 %
19 %
8 %
0.1 %
0.3 %
4 %
6 %
37 %
10 %
0 %
0.3 %
8 %
0.6 %
42 %
CD11b
CD14
CD103
Ly-6C
CCR7-GFP
b
Ccr7+/+
Ccr7gfp/+
CCR7-GFP+ in subsets (%)
75
50
25
0
CD11bhi
CD14hi
CD103+
Ly-6Chi
c
pre-culture
day 4
day 7
d
I-A
CD11c
CD11b
CD115
e
day 4
day 7
Ccr7+/+
Ccr7gfp/+
0.1 %
0.4 %
6 %
10 %
CD14
CCR7-GFP

Supplementary Figure S4. *Ccr7-gfp* expression in moDCs from skin-draining LNs and in bone marrow monocytes-derived DCs. (**a**) Cytograms showing *Ccr7-gfp* expression in $CD11c^{+}I\text{-}A^{+}$ DCs isolated from skin-draining LNs 24 h after i.v. injection of LPS. (**b**) Compiled data of $CCR7\text{-}GFP^{+}$ cells in the indicated subpopulations of DCs from skin-draining LNs (n=3). (**c-e**) Bone marrow monocyte-derived DCs. $Ly\text{-}6C^{hi}CD11b^{hi}$ inflammatory monocytes were purified from bone marrow and cultured for up to 7 days in media containing GM-CSF and IL-4. (**c**) Representative images of cells after the indicated number of culture days photographed with a 40x objective. (**d**) Surface marker display of cells after 4 days of culture. (**e**) *Ccr7-gfp* expression in cells after 4 or 7 days of culture.

Figure S5

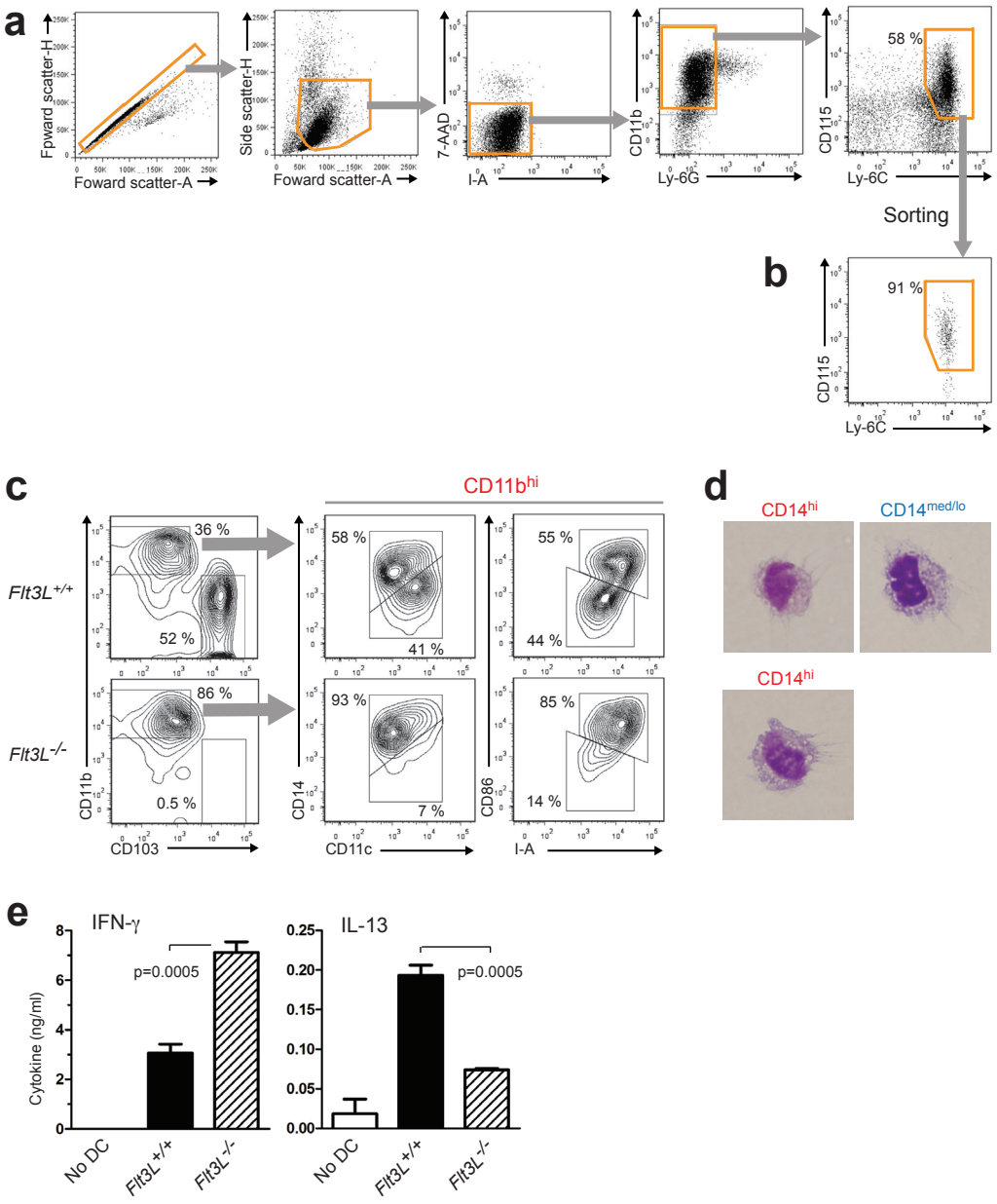
a
Fpward scatter-H
Foward scatter-A
Side scatter-H
Foward scatter-A
7-AAD
I-A
CD11b
Ly-6G
CD115
58 %
Ly-6C
Sorting
b
91 %
CD115
Ly-6C
c
CD11b^hi
Flt3L+/+
Flt3L-/-
36 %
52 %
86 %
0.5 %
CD11b
CD103
58 %
41 %
93 %
7 %
CD14
CD11c
55 %
44 %
85 %
14 %
CD86
I-A
d
CD14^hi
CD14^med/lo
CD14^hi
e
IFN-γ
p=0.0005
IL-13
p=0.0005
Cytokine (ng/ml)
No DC
Flt3L+/+
Flt3L-/-
No DC
Flt3L+/+
Flt3L-/-

Supplementary Figure S5. Purification of bone marrow monocytes and analysis of lung CD11b^{hi} DCs in *Flt3L*$^{-/-}$ mice. (**a**) Gating strategy for CD11b^{+}CD115^{+}Ly-6C^{hi} monocyte purification by flow cytometry. CD11c^{+}, I-A^{+}, and Ly-6G^{+} cells were depleted by magnet activated cell sorter prior to flow cytometry-based cell sorting. (**b**) Purity of CD115^{+}Ly-6C^{hi} monocytes after cell sorting. (**c**) FACS profiles of lung DC subsets in wild-type and *Flt3L*$^{-/-}$ mice. CD11b^{hi} DCs were further analyzed with CD14 and CD11c staining, and I-A and CD86 staining. (**d**) Images of CD14^{hi}CD11c^{int} DCs and CD14$^{med/lo}$CD11c^{hi} DCs from lung of wild-type or *Flt3L*$^{-/-}$ mice photographed using a 60x objective lens. (**e**) Th1 and Th2 differentiation of naïve T cells induced by lung DCs. Wild-type and *Flt3L*$^{-/-}$ mice were instilled with OVA/LPS and lungs excised 16 h later. CD11c^{+}I-A^{+}autofluorescence^{lo} total DCs were purified by flow cytometry then cultured with OVA-specific OT-II CD4^{+} T cells for 5 days. T cell responses were elicited by the incubation of cultured T cells in an anti-CD3ε and anti-CD28 mAb-coated plate for 24 h. IFN-γ and IL-13 in the supernatants were measured by ELISA to estimate Th1 and Th2 differentiation, respectively.